J|A|C|S
COMMUNICATIONS

Published on Web 12/15/2006

Mammalian Cell Surface Imaging with Nitrile-Functionalized Nanoprobes: Biophysical Characterization of Aggregation and Polarization Anisotropy in SERS Imaging

Qingyan Hu,[†] Li-Lin Tay,*[,‡] Matthew Noestheden,[†] and John Paul Pezacki*[,†]

Steacie Institute for Molecular Sciences and Institute for Microstructural Sciences, National Research Council Canada, Ottawa, Ontario, Canada K1A 0R6

Received September 29, 2006; E-mail: lilin.tay@nrc-cnrc.gc.ca; john.pezacki@nrc-cnrc.gc.ca

Recently, Raman and surface enhanced Raman scattering (SERS) spectroscopies have been applied to biosensing, as they offer high information content about the analyte.[1] Nanoparticle-based SERS techniques have proven to be excellent methods for sensing DNA hybridization[2] and protein binding events.[3] However, Raman and SERS microscopies have seen limited applications in biological imaging. Although high-resolution Raman microscopy yields high information content cellular images, this technique is plagued by poor scattering cross sections, which results in lengthy acquisition times and high excitation power. The SERS effect, which is due primarily to the enhancement of the electromagnetic field associated with strong/localized surface plasmon resonances near the surface of nanostructure assemblies,[4] allows for greater sensitivity. Colloidal gold or silver nanoparticles (NPs) are popular SERS active platforms in most biological studies.[3,5]

An important frontier in molecular imaging is the utilization of the enormous sensitivity of SERS to achieve specific detection of cellular proteins in vivo.[6] Very often proteins give rise to spectrally complex finger print regions. This, coupled with the spectral fluctuations inherent to SERS, makes the identification of specific protein species extremely challenging. Therefore, we have designed a biomolecular Raman label with a Raman signature that is unique compared with those of cellular materials. Furthermore, our Raman label possesses orthogonal functionality and is chemically inert under live cell imaging conditions. We report here silver NPs (Ag-NPs) with a ligand containing a cyano group as a Raman reporter **1** (Figure 1a). The syntheses of **1** and Ag-NPs coated with **1** (Ag-NP-**1**) are in the Supporting Information. The unique vibrational mode of the C≡N stretch was used for vibrational contrast in cellular imaging experiments. The probe molecule also has a terminal hydrazide to achieve specific labeling of ketones conjugated to cell surface proteins. We successfully labeled HeLa cells expressing the transmembrane domain of the platelet-derived growth factor receptor (TM) with Ag-NP-**1** using the method established by Ting and co-workers (see Supporting Information).[7]

Figure 1c shows an optical image of a HeLa cell transfected with TM containing an acceptor peptide (AP) tag that was subsequently labeled with a ketone analogue of biotin[7] and Ag-NP-**1**. Its corresponding Raman intensity map from the CN vibration band is depicted in Figure 1d. In the Raman map, three intense spots (I, II, and III) are identified, and their corresponding Raman spectra are shown in Figure 1b. Both spectra I and II exhibit obvious C≡N bands at 2230 cm^{-1}. A much weaker C≡N stretch was observed at spot III. Intensity contrasts between the three SERS hot-sites and regions without Ag-NPs are ~3 orders of magnitude. Inset of Figure 1b is a typical cellular Raman spectrum obtained from spot IV of the same cell but in a region without Ag-NP-**1**

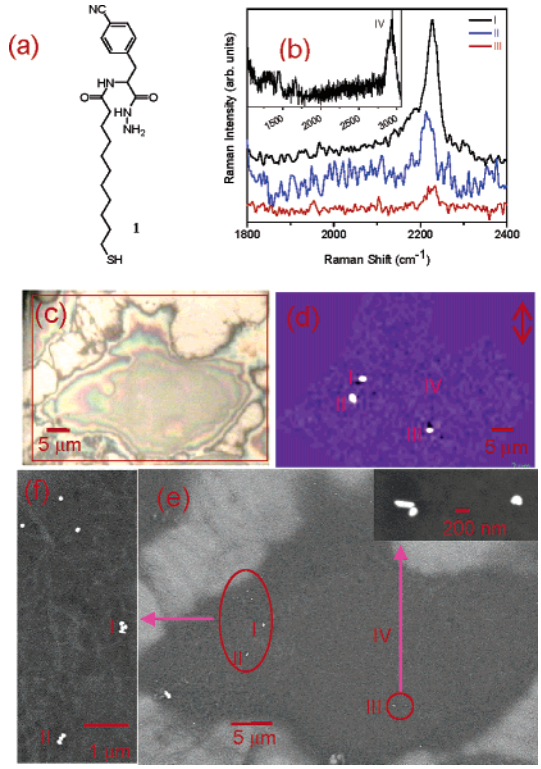

Figure 1. (a) The chemical structure of Raman reporter **1**; (b) Raman spectra of the CN vibration mode extracted from positions I, II, and III of the cell shown in the optical image (c). Inset of (b) is a cellular Raman spectrum taken from spot IV of the same cell. (d) Raman intensity map of the C≡N band of the same cell, and (e) the corresponding SEM image. Inset in (e) showed the NPs in the lower right circle. (f) The group of NPs as shown in the large oval of (e).

(Figure 1d). This cell spectrum consists of the following bands: 1660 (amide I), 1447 (CH_2, CH_3), 1285 and 1350 (amide III, NH, CH), and 2990 (CH) cm^{-1}.[8]

Membrane proteins often cluster onto microdomains called rafts, which may help facilitate aggregation of NPs upon labeling. Scanning electron microscopy (SEM) was performed on the same cell to correlate the observed SERS hot-sites with the presence of anchored NPs (Figure 1e). The SEM image revealed several NPs. The inset of Figure 1e shows a pair of NPs located at the bottom of the cell that consist of a single NP and a dimerized NP composed of a nanorod and a spherical NP. Figure 1f shows the magnification of the larger group of NPs encircled in Figure 1e (large oval). Again, the NPs identified in Figure 1f are made of small NP aggregates (tetramer and trimer) and a few monomers. Comparing the SEM images to the Raman intensity plot facilitated the assignment of the NP aggregates responsible for all the observed intense SERS

[†] Steacie Institute for Molecular Sciences.
[‡] Institute for Microstructural Sciences.

10.1021/ja0670005 CCC: $37.00

hot-spots in Figure 1d. Strong SERS signals observed at spots I, II, and III were generated by tetramer, trimer, and dimer NPs, respectively. Although the SEM image (Figure 1e) also revealed another Ag aggregate located at the lower left of the cell, careful examination of this cluster with SEM showed that the Ag cluster is actually embedded inside the cell. Raman spectra taken from this region do show enhancement, although much weaker in intensity (~50-fold) compared with those aggregates located on the cell surface. Moreover, repeated cell surface labeling with Ag-NP-**1** indicated that only nanoparticle aggregates (dimers or greater) showed measurable SERS signals. Generally, the SERS enhancement factor is about 10^{10} (see Supporting Information).

Theoretical calculations have shown that SERS enhancement factors from isolated NPs are orders of magnitude smaller than those of aggregated NPs.[9] The SERS enhancement factor of a dimerized NP increases dramatically when the molecule of interest is situated in the interstitial gap of the dimer NPs,[9,10] implying that enhancement depends strongly on the interstitial gap between the NPs. With an interstitial gap of ~5 nm, the SERS enhancement factor can exceed 6 orders of magnitude and 10 orders of magnitude with a 1 nm interstitial gap.[11] Trimers and other smaller NP aggregates can be treated as ensembles of coupled dimer systems and therefore can produce extremely intense SERS hot-sites provided sufficiently small interstitial gaps are present. Although single NPs are capable of field enhancement, their SERS intensity is simply too weak to be observed in our imaging experiments.

We also observed that aggregated NPs exhibit strong polarization anisotropy. Particles identified in the SEM images labeled as spots I, II, and III (Figure 1e) all have their interparticle axes oriented largely parallel to the incident electric field. This relationship is necessary to achieve a capacitive field enhancement and hence generate intense SERS hot-sites.[4,10] If the incident light polarization is perpendicular to the interparticle axes of the aggregated NPs, the exclusion of the field between the NPs results in no enhancement (see Supporting Information).

As the Raman images were obtained by rastering cells under a tightly focused incident beam, light-induced damage is a legitimate concern. To investigate this problem, we observed SEM images of several cells before and after Raman imaging (Figure 2a). The Raman and SEM image of a representative cell showed excellent correlation between the locations of SERS and aggregated Ag-NP-**1**. The same cell was examined under SEM after Raman imaging. We observed localized rupturing of the cell membrane under several aggregated Ag-NP-**1** (Figure 2c,d) and a NP monomer (Figure 2b). These results indicated that damage at NP aggregates was the most extensive. Supporting this was the finding that, when we reduced the imaging power density by 1 order of magnitude, no detectable membrane damage was observed. Similar NP-induced photothermal effects to cells have been reported[12] and often result in irreparable damage to cells.

In summary, we have demonstrated imaging of membrane proteins on cells using a cyano-labeled SERS probe. Observed SERS hot-sites correlate well with small aggregated NPs. Furthermore, the strongest SERS signals originate from aggregates oriented in the appropriate direction with respect to the incident laser polarization. These observations are critical for the design of future molecular imaging agents for SERS imaging of cells and tissues. Fortuitously, many cell surface receptors function as clusters which may help to facilitate NP aggregation and orientation in cellular and tissue imaging experiments.[13] We are currently pursuing such imaging studies.

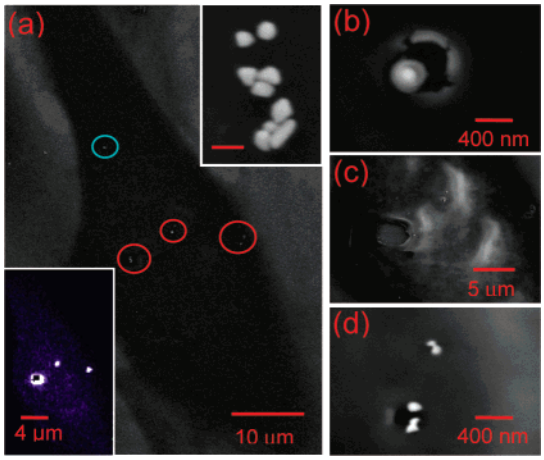

Figure 2. (a) SEM image of a cell. Upper right inset: magnification of a group of aggregated NPs. The scale bar is 200 nm. Lower left inset: the corresponding Raman intensity image of the same cell obtained with a power density of 10^5 W/cm^2. Laser-induced damage to the cell is shown in (b) the monomer (blue circle in a), (c) the aggregates, and (d) a pair of dimers.

Acknowledgment. We thank Prof. Alice Ting at MIT for providing biotin ketone, as well as the AP-CFP-TM and BirA plasmids. We gratefully acknowledge the help of Mr. Jeff Fraser for SEM imaging, and Dr. Jean Lapointe for fabricating the patterned Si substrate.

Supporting Information Available: Experimental details and information on polarization anisotropy. This material is available free of charge via the Internet at http://pubs.acs.org.

References

(1) (a) Petry, R.; Schmitt, M.; Popp, J. *ChemPhysChem* **2003**, *4*, 4−30. (b) Campion, A.; Kambhampati, P. *Chem. Soc. Rev.* **1998**, *27*, 241−250.
(2) (a) Cao, Y. C.; Jin, R.; Mirkin, C. A. *Science* **2002**, *297*, 1536−1540. (b) Cao, Y. C.; Jin, R.; Nam, J.-M.; Thaxton, C. S.; Mirkin, C. A. *J. Am. Chem. Soc.* **2003**, *125*, 14676−14677.
(3) (a) Delfino, I.; Bizzarri, A. R.; Cannistraro, S. *Biophys. Chem.* **2005**, *113*, 41−51. (b) Ruan, C. M.; Wang, W.; Gu, B. H. *Anal. Chem.* **2006**, *78*, 3379−3384.
(4) (a) Moskovits, M. *Rev. Mod. Phys.* **1985**, *57*, 783−826. (b) Moskovits, M. *J. Raman Spectrosc.* **2005**, *36*, 485−496.
(5) (a) Premasiri, W. R.; Moir, D. T.; Klempner, M. S.; Krieger, N.; Jones, G.; Ziegler, L. D. *J. Phys. Chem. B* **2005**, *109*, 312−320. (b) Kneipp, J.; Kneipp, H.; Rice, W. L.; Kneipp, K. *Anal. Chem.* **2005**, *77*, 2381−2385. (c) Zeiri, L.; Efrima, S. *J. Raman Spectrosc.* **2005**, *36*, 667−675.
(6) (a) Souza, G. R.; Christianson, D. R.; Staquicini, F. I.; Ozawa, M. G.; Snyder, E. Y.; Sidman, R. L.; Miller, J. H.; Arap, W.; Pasqualini, R. *Proc. Natl. Acad. Sci. U.S.A.* **2006**, *103*, 1215−1220. (b) Kneipp, J.; Kneipp, H.; Rice, W. L.; Kneipp, K. *Anal. Chem.* **2005**, *77*, 2381−2385.
(7) Chen, I.; Howarth, M.; Lin, W.; Ting, A. Y. *Nat. Methods* **2005**, *2*, 99−104.
(8) (a) Puppel, G. J.; De Mul, F. F. M.; Otto, C.; Greve, J.; Robert-Nicoud, M.; Arndt-Jovin, D. J.; Jovin, T. M. *Nature* **1990**, *347*, 301−303. (b) Peticolas, W. L.; Patapoff, T. W.; Thomas, G. A.; Postlewait, J.; Powell, J. W. *J. Raman Spectrosc.* **1996**, *27*, 571−578.
(9) Xu, H. X.; Bjerneld, E. J.; Kall, M.; Borjesson, L. *Phys. Rev. Lett.* **1999**, *83*, 4357−4360.
(10) Bosnick, K. A.; Jiang, J.; Brus, L. *J. Phys. Chem. B* **2002**, *106*, 8096−8099.
(11) Jiang, J.; Bosnick, K. A.; Maillard, M.; Brus, L. *J. Phys. Chem. B* **2003**, *107*, 9964−9972.
(12) Loo, C.; Lowery, A.; Halas, N.; West, J.; Drezek, R. *Nano Lett.* **2005**, *5*, 709−711.
(13) Ianoul, A.; Grant, D. D.; Rouleau, Y.; Bani-Yaghoub, M.; Johnston, L. J.; Pezacki, J. P. *Nat. Chem. Biol.* **2005**, *1*, 196−202.

JA0670005